

X-ray Powder Diffraction Study of Organometallic Polymers: $[\text{Ru}(\text{L})(\text{CO})_2]_n$ (L = 2,2'-Bipyridine or 1,10-Phenanthroline)

Norberto Masciocchi,[†] Angelo Sironi,^{*,‡} Sylvie Chardon-Noblat,[§] and Alain Deronzier[§]

Dipartimento di Scienze Chimiche Fisiche e Matematiche, Università dell'Insubria, via Valleggio 11, 22100 Como, Italy, Dipartimento di Chimica Strutturale e Stereochimica Inorganica, Università di Milano, via G. Venezian 21, 20133 Milano, Italy, and Laboratoire d'Electrochimie Organique et de Photochimie Rédox, UMR CNRS 5630, Université Joseph Fourier, BP53, 38041 Grenoble, Cedex 9, France

Received April 16, 2002

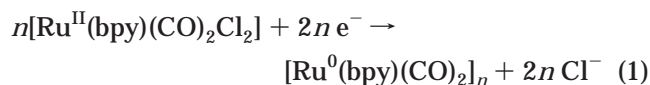
Summary: A combination of rather unconventional XRPD methods has been used to assess the polymeric nature of the $[\text{Ru}(\text{L})(\text{CO})_2]_n$ (L = 2,2'-bipyridine, 4,4'-dimethyl-2,2'-bipyridine, and 1,10-phenanthroline) derivatives. The polymeric chains pack pseudohexagonally in the ab plane and grow along c with Ru–Ru distances close to 3.0 Å. The very poor diffraction patterns of these electrogenerated polymers suggest that the flat $\text{Ru}(\text{L})(\text{CO})_2$ monomers are staggered by 45° or 135° rotations (as in $[\text{Ru}(\text{CO})_4]_n$) but stack in random sequence along the chains.

Introduction

Examples of polymers based on metal–metal bond chains expected to exhibit unusual properties (catalytic, conductivity, photochemistry) are rare.¹ In this context, we have developed, over a few years, a novel type of organometallic polymer based on chains of ruthenium atoms. The low metal oxidation state $[\text{Ru}(0)]$ and the two vacant coordination sites needed for the metal chain formation can be easily achieved by an electrochemical procedure.² For instance, the two-electron reduction, either of a mononuclear complex of $\text{Ru}(\text{II})$, $[\text{Ru}(\text{bpy})(\text{CO})_2\text{Cl}_2]$ (bpy = 2,2'-bipyridine), or of a $\text{Ru}(\text{I})$ dimer like $[\text{Ru}(\text{bpy})(\text{CO})_2(\text{CH}_3\text{CN})]_2(\text{PF}_6)_2$,³ is associated with the loss of two labile ligands (chloride or acetonitrile, respectively).

This original principle has been successfully applied to the preparation of a large variety of $[\text{Ru}(\text{L})(\text{CO})_2]_n$ redox active polymers (L = bidentate nitrogen ligands, especially 2,2'-bipyridine and 1,10-phenanthroline derivatives).^{2,4} These materials can be easily prepared as adherent “crystalline” thin films on conductive supports

by an electroreduction process. Equation 1 summarizes the overall electropolymerization process involved for e.g. $[\text{Ru}(\text{bpy})(\text{CO})_2\text{Cl}_2]$.



Polymers such as these proved to be highly selective and efficient electrocatalysts for the reduction of carbon dioxide in pure aqueous media⁵ and also for the water gas shift reaction.⁶ They also exhibit interesting photochemical properties.⁷ Furthermore, a similar redox-active polymer of osmium has been prepared very recently following a similar approach,⁸ demonstrating that this electrochemical process could contribute to the construction of polymer films with other metal centers.

The high insolubility of these polymers in most common solvents and their air-sensitivity prevent the full characterization and particularly the growth of single crystals for X-ray analysis and then the determination of their precise structure. Up to now the proposed molecular structure of these polymers has been strongly supported by detailed physicochemical analysis in the solid state (electrochemistry, elemental analysis, FAB MS, UV–vis, and IR spectroscopy). All the data thus obtained emphasized that the polymers are based on metal–metal bond chains.²

Nowadays, the structure determination problem can be circumvented in some cases by attempting an ab initio X-ray powder diffraction (XRPD) structure determination.⁹ This technique has been previously applied with success to solve the structure of some simple

* Address correspondence to this author. E-mail: a.sironi@csmto.mi.cnr.it. Fax: 39-02-50314454.

[†] Università dell'Insubria.

[‡] Università di Milano.

[§] Université Joseph Fourier.

(1) Nguyen, P.; Gómez-Elipé, P.; Manners, I. *Chem. Rev.* **1999**, *99*, 1515 and references therein.

(2) Chardon-Noblat, S.; Deronzier, A.; Ziessel, R. *Collect. Czech. Chem. Commun.* **2001**, *66*, 207 and references therein.

(3) Chardon-Noblat, S.; Cripps, G. H.; Deronzier, A.; Field, J. S.; Gouws, S.; Haines, R. J.; Southway, F. *Organometallics* **2001**, *20*, 1668.

(4) Caix-Cecillon, C.; Chardon-Noblat, S.; Deronzier, A.; Haukka, M.; Pakkanen, T. A.; Ziessel, R.; Zsoldos, D. *J. Electroanal. Chem.* **1999**, *466*, 187.

(5) (a) Collomb-Dunand-Sauthier, M.-N.; Deronzier, A.; Ziessel, R. *J. Chem. Soc., Chem. Commun.* **1994**, 189. (b) Collomb-Dunand-Sauthier, M.-N.; Deronzier, A.; Ziessel, R. *Inorg. Chem.* **1994**, *33*, 2961. Chardon-Noblat, S.; Collomb-Dunand-Sauthier, M.-N.; Deronzier, A.; Ziessel, R.; Zsoldos, D. *Inorg. Chem.* **1994**, *33*, 4410. Chardon-Noblat, S.; Deronzier, A.; Ziessel, R.; Zsoldos, D. *J. Electroanal. Chem.* **1998**, *444*, 253.

(6) Luukkanen, S.; Homanen, P.; Haukka, M.; Pakkanen, T. A.; Deronzier, A.; Chardon-Noblat, S.; Zsoldos, D.; Ziessel, R. *Appl. Catal. A* **1999**, *185*, 157.

(7) Eskelinen, E.; Haukka, M.; Venäläinen, T.; Pakkanen, T. A.; Wasberg, M.; Chardon-Noblat, S.; Deronzier, A. *Organometallics* **2000**, *19*, 163.

(8) Chardon-Noblat, S.; Deronzier, A.; Hartl, F.; Van Slageren, J.; Mahabriesing, T. *Eur. J. Inorg. Chem.* **2001**, 613.

organometallic polymers, like $[\text{Ru}(\text{CO})_4]_n$,¹⁰ $\{\text{Re}(\mu\text{-H})(\text{CO})_4\}_n$,¹¹ or $[\text{PdCl}(\text{CH}_2\text{COCH}_3)]_n$.¹²

In this paper we exploit XRPD (and the known structure of $[\text{Ru}(\text{CO})_4]_n$) to infer the structures of $[\text{Ru}(\text{L})(\text{CO})_2]_n$ [$\text{L} = 2,2'$ -bipyridine (bpy), 4,4'-dimethyl-2,2'-bipyridine (dmbpy), 1,10-phenanthroline (phen)] and to demonstrate their truly polymeric nature.

Experimental Section

General Methods. Supporting electrolyte Bu_4NClO_4 (TBAP), collodion, amyl acetate from Fluka, and CH_3CN from Rathburn (HPLC grade) were used as received. Electrochemical experiments were made with an EG&G Princeton Applied Research model 173 potentiostat galvanostat. Polymerizations were run in a conventional three-electrode cell under an argon atmosphere in a dry glow box (JARAM). The working electrode was a slide/SiO₂/SnO₂/F⁻, the auxiliary electrode a platinum wire in $\text{CH}_3\text{CN} + 0.1 \text{ M TBAP}$, and the reference electrode an Ag/10 mM Ag⁺ in $\text{CH}_3\text{CN} + 0.1 \text{ M TBAP}$.

Synthesis. The $[\text{Ru}(\text{bpy})(\text{CO})_2]_n$ polymer was grown by a controlled potential reduction either of a 2 mM solution of *trans*-(Cl)[Ru(bpy)(CO)₂Cl₂]¹³ ($E_{\text{app}} = -1.65 \text{ V}$) Ru(II) monomer or of a solution of *trans*-(CH₃CN)-[Ru(bpy)(CO)₂(CH₃CN)]₂-(PF₆)₂ Ru(I) dimer³ ($E_{\text{app}} = -1.40 \text{ V}$) in $\text{CH}_3\text{CN} + 0.1 \text{ M TBAP}$ on a conductive support consisting of a 15 × 15 mm² slide coated with SiO₂/SnO₂ doped by fluorine (Glastron). The concentration of Ru atoms on the substrate surface was calculated from the quantity of electricity consumed during the polymerization ($\Gamma_{\text{Ru}} \approx 10^{-5} \text{ mol/cm}^2$). After being washed with a few milliliters of CH_3CN , the film was stabilized by depositing a few droplets of a solution made from 5% collodion in amyl acetate on the sample and dried under vacuum for 3 h. Most of the XRPD data were collected directly on the modified substrate (see below). The corresponding $[\text{Ru}(\text{L})(\text{CO})_2]_n$ polymers with $\text{L} = \text{dmbpy}$ or phen were prepared according to the same procedures.

X-ray Powder Diffraction Studies. X-ray diffraction data of $[\text{Ru}(\text{bpy})(\text{CO})_2]_n$ were collected on powders deposited on a quartz zero-background plate with the aid of a binder (5% collodion in amyl acetate), using a Philips PW1820 vertical-scan diffractometer, equipped with a Cu tube ($\lambda = 1.5418 \text{ \AA}$) and a graphite monochromator and Soller slits in the diffracted beam. The generator was operated at 40 kV and 40 mA. Slits used: DS 1.0°; RS 0.2 mm. Data were collected in the $5 < 2\theta < 55^\circ$ range, with $t = 5 \text{ s}$ and $\Delta 2\theta = 0.02^\circ$. For the remaining species, XRPD data were collected directly on the as-prepared films electrochemically grown on the slide/SiO₂/SnO₂/F⁻ electrodes.

As shown in Figure 1, all specimens gave very poor diffraction patterns, mostly characterized by an intense broad peak centered at about $2\theta < 10^\circ$, and by few (much weaker) subsidiary peaks below 40° (2θ); additional narrow peaks are observed in the thin films patterns, which are attributed to the crystalline SiO₂/SnO₂/F⁻ substrate (isomorphous to cassiterite). Obviously, traditional indexing and ab initio structure solution approaches from XRPD data could not be performed on these poorly crystalline species; therefore, unit-cell determination and model-building techniques had to be performed "manually", taking advantage of chemical, spectroscopic, and

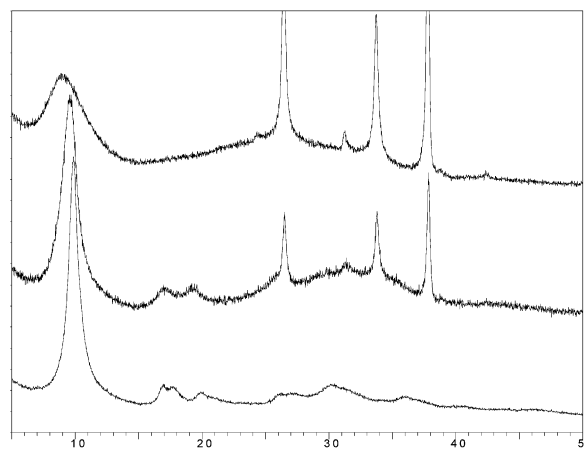


Figure 1. Raw diffraction data for the $[\text{Ru}(\text{bpy})(\text{CO})_2]_n$, $[\text{Ru}(\text{phen})(\text{CO})_2]_n/\text{SiO}_2/\text{SnO}_2/\text{F}^-$, and $[\text{Ru}(\text{dmbpy})(\text{CO})_2]_n/\text{SiO}_2/\text{SnO}_2/\text{F}^-$ species (bottom to top). In the last two patterns, SiO₂/SnO₂/F⁻ peaks from the substrate are clearly visible as sharp reflections. Horizontal scale 2θ (deg).

structural evidence available from analogous oligomeric compounds. Among the collected patterns, the one showing the narrowest peaks (of typical 1.2° fwhm) was that of the $[\text{Ru}(\text{bpy})(\text{CO})_2]_n$ species, which was then used to build a *very rough* "structural model", as described in the following:

(a) We observed that the major peak locations [with $(d^*)^2$ -value ratios of approximately 1:3:4:7] could be interpreted by a two-dimensional hexagonal lattice [for which $d^* \propto (h^2 + k^2 + hk)^{1/2}$] with $a = 10.2 \text{ \AA}$, or in an alternative, but equivalent, by a centered rectangular lattice with $a = 10.2 \text{ \AA}$ and $b = \sqrt{3}a = 17.66 \text{ \AA}$.

(b) Splitting of all peaks (including the intense one, which shows a non-negligible high-angle tail), however, indicated a lower symmetry, consistent, accordingly to a Le-Bail peak-fitting procedure, with a centered rectangular lattice with $a = 10.4 \text{ \AA}$ and $b = 16.8 \text{ \AA}$.

(c) The third dimension (if any) of the average lattice was estimated to be close to 3 Å, and responsible for the broad feature observed near $2\theta = 30^\circ$. Thus a C-centered orthorhombic lattice was assumed on the basis of the systematic absences, while the *Cmmm* space group was chosen upon stereochemical considerations.

(d) The intramolecular features of the $[\text{Ru}(\text{bpy})(\text{CO})_2]$ monomer were modeled by a planar C_{2v} fragment, built upon literature values of similar molecules.

(e) Volume considerations unambiguously led to a $Z = 2$ value. Accordingly, the unique Ru atom must sit, in *Cmmm*, in (or near) 0,0,0, and the whole molecule lies in the $z = 0$ plane. This observation alone allows the nature of the polymer to be inferred, where chains of collinear Ru atoms run parallel to [001], at a distance determined by the c parameter.

(f) Moreover, the space group symmetry indicates that the monomer is necessarily disordered about the *mmm* position, its rotation about the c axis (R_z) being undefined by symmetry. Therefore, the crystallographic task in our hands shrinks to the determination of such an R_z value of a *rigid* monomer, to the estimation of the intermolecular interactions, and to the crystallochemical, i.e. *structural*, interpretation of the derived model.

(g) To determine the most plausible R_z value, we used the simulated-annealing features of the highly performing TOPAS-R program,¹⁴ which was eventually employed also to refine the final model with the aid of the fundamental parameter approach and of the anisotropic model for the ($\cos \theta$ dependent) small-particle-size broadening. A single isotropic

(9) (a) Harris, K. D. M.; Tremayne, M. *Chem. Mater.* **1996**, *8*, 2554. (b) Langford, J. I.; Louër, D. *Rep. Prog. Phys.* **1996**, *59*, 131. (c) Poojary, D. M.; Clearfield, A. *Acc. Chem. Res.* **1997**, *30*, 414. (d) Masciocchi, N.; Sironi, A. *J. Chem. Soc., Dalton Trans.* **1997**, 4643.

(10) Masciocchi, N.; Moret, M.; Cairati, P.; Ragaini, F.; Sironi, A. *J. Chem. Soc., Dalton Trans.* **1993**, 471.

(11) Masciocchi, N.; D'Alfonso, G.; Garavaglia, L.; Sironi, A. *Angew. Chem., Int. Ed.* **2000**, *39*, 4478.

(12) Masciocchi, N.; Ragaini, F.; Sironi, A. *Organometallics* **2002**, *21*, 3489.

(13) Chardon-Noblat, S.; Da Costa, P.; Deronzier, A.; Haukka, M.; Pakkanen, T. A.; Ziessel, R. *J. Electroanal. Chem.* **2000**, *490*, 62.

(14) Bruker AXS 2000: Topas V2.0: General profile and structure analysis software for powder diffraction data.

Table 1. Crystal Data, and Details on Refinement for [Ru(bpy)(CO)₂]_n and [Ru(phen)(CO)₂]_n/SiO₂/SnO₂/F⁻

	[Ru(bpy)(CO) ₂] _n	[Ru(phen)(CO) ₂] _n
formula	C ₁₂ H ₈ N ₂ O ₂ Ru	C ₁₄ H ₈ N ₂ O ₂ Ru
method	XRPD	XRPD
system	orthorhombic	orthorhombic
space group	<i>Cmmm</i>	<i>Cmmm</i>
<i>a</i> , Å	16.75	18.72
<i>b</i> , Å	10.38	10.68
<i>c</i> , Å	2.95	2.94
<i>Z</i>	2	2
fw, g mol ⁻¹	313.27	337.28
<i>V</i> , Å ³	514	587
ρ_{calcd} , g cm ⁻³	2.02	1.91
<i>F</i> (000)	308	332
diffractometer	Philips PW1820	Philips PW1820
<i>T</i> , K	298	298
2 θ range, deg	5–55	5–85
<i>N</i> _{data}	2501	4001
<i>N</i> _{obs}	44	151
<i>R</i> _p , <i>R</i> _{wp}	0.034, 0.043	0.044, 0.057
χ	2.02	1.38

^a $R_p = \sum_i |y_{i,o} - y_{i,c}| / \sum_i |y_{i,o}|$; $R_{wp} = [\sum_i w_i (y_{i,o} - y_{i,c})^2 / \sum_i w_i (y_{i,o})^2]^{1/2}$; $\chi^2 = \sum_i w_i (y_{i,o} - y_{i,c})^2 / (N_{\text{obs}} - N_{\text{data}})$, where $y_{i,o}$ and $y_{i,c}$ are the observed and calculated profile intensities, respectively. The summations run over *i* data points. Statistical weights w_i are normally taken as $1/y_{i,o}$.

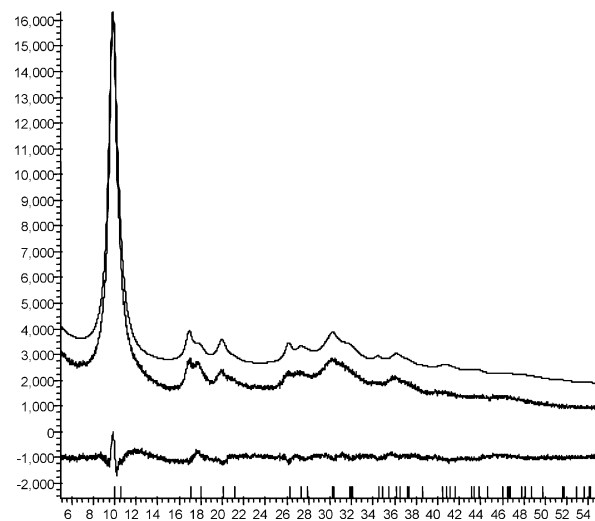
thermal parameter was used, with the Ru atom allowed to lie off the origin (of *mmm* site symmetry). Summary crystal data and experimental details can be found in Table 1. The final Rietveld refinement plot with peak markers is shown in Figure 2a. The list of the refined parameters comprises lattice parameters, background polynomial, peak shape and width, a specimen displacement parameter, and rigid group location and orientation (x, y, R_z).

(h) Visual inspection of the diffraction data and model optimization of a rigid [Ru(phen)(CO)₂] monomer allowed indexing of the pattern and determination of a highly disordered (*hexagonal or very nearly so*) *P6/mmm* crystal structure, which shares the basic features, when described in *Cmmm*, of [Ru(bpy)(CO)₂]_n. Table 1 and Figure 2b also contain the relevant data for [Ru(phen)(CO)₂]_n.

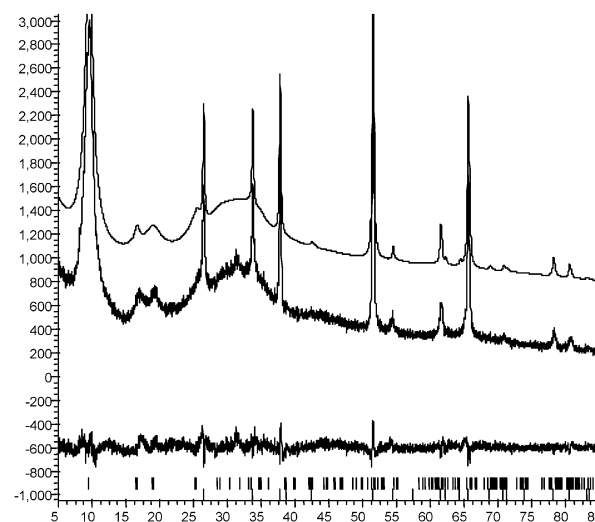
Results and Discussion

As discussed in the Experimental Section we have tackled this structure determination by a rather unusual approach. Indeed, the poor crystallinity of our samples prevents “automatic” indexing and conventional structure solution. However, the knowledge of the structure of [Ru(CO)₄]_n has allowed us to build a model of pseudohexagonally packed chains and to derive the corresponding set of cell parameters. The correctness of this choice is further corroborated by a number of experimental evidences, by their internal coherence, and by their consistency with our structural model.

The simplest and “best” crystallized species is [Ru(bpy)(CO)₂]_n, which has an orthorhombic cell with *Z* = 2 and contains a 2D arrangement of flat molecules (lying at *z* = 0, see Figure 3) stacked as to generate “infinite” chains running along *c*. [Ru(phen)(CO)₂]_n is much more badly crystallized while [Ru(dmbpy)(CO)₂]_n has basically no Bragg peaks (see Figure 1); nevertheless, a similar model can be envisaged for both derivatives. Consistently, the positions of the most prominent peak in the [Ru(bpy)(CO)₂]_n, [Ru(phen)(CO)₂]_n, and [Ru(dmbpy)(CO)₂]_n species is related to the area of the 2D lattice and, thanks to the similar thickness of the monomers,



(a)



(b)

Figure 2. Final Rietveld refinement plots for [Ru(bpy)(CO)₂]_n (a) and [Ru(phen)(CO)₂]_n/SiO₂/SnO₂/F⁻ (b) with peak markers and difference plot at the bottom. The offset of the two curves has been obtained by adding an arbitrary (constant) value to the refined background contribution. Horizontal scale 2 θ (deg).

correlate well with the volume of the ligands (estimated with SMILE,¹⁵ see Figure 4). The fingerprint of the third dimension (the *c* axis) is the bump occurring at ca. 28–30° in all three patterns, which is related to a Ru–Ru distance near 3.0 Å. Such a short translation period *does not mean* that each molecule is eclipsed with those above and below in the chain. In fact, the monomer is disordered about a *mmm* site with four equivalent orientations (at ca. +45°, –45°, +135°, and –135° to each other) which randomly alternate throughout the chain (see Figure 5). Staggering thus minimizes all interactions along *z* between neighboring molecules. According to the Cambridge Data File, a staggering of $\pm 135^\circ$ is slightly more common than the $\pm 45^\circ$ torsion. If only $\pm 135^\circ$ rotations were randomly present along a chain, the XRPD pattern would be identical, thus

(15) Eufri, D.; Sironi, A. *J. Mol. Graphics* **1989**, *7*, 165.

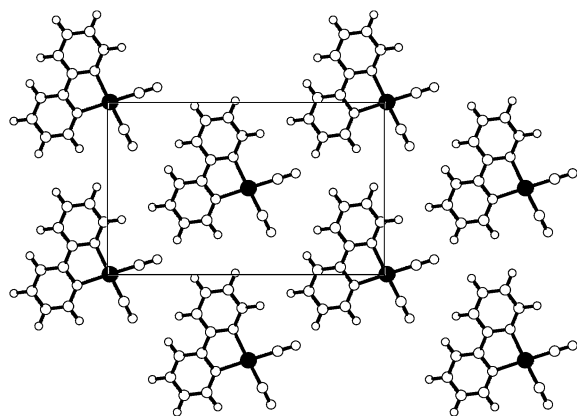


Figure 3. Crystal packing in the $z = 0$ plane for the pseudo-hexagonally packed $[\text{Ru}(\text{bpy})(\text{CO})_2]$ monomers. The Ru–Ru bonds run normal to this plane. Shortest intermolecular contacts are C–H \cdots O bonds of ca. 2.75 Å. For the sake of simplicity, the picture has been drawn in the ordered cI plane group; however, according to the disorder observed in the actual $Cmmm$ space group (see text), for each monomer four distinct (mirror related) orientations are present in the crystal.

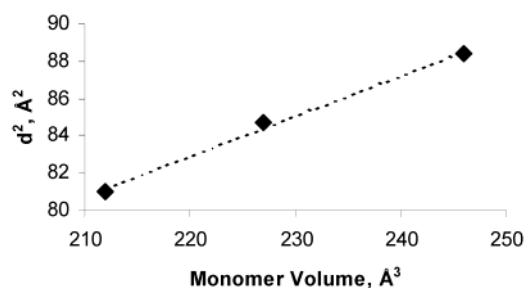


Figure 4. Plot of molecular observed d spacing squared (Å^2) for the most prominent XRPD and the monomer volume (Å^3), estimated by SMILE.

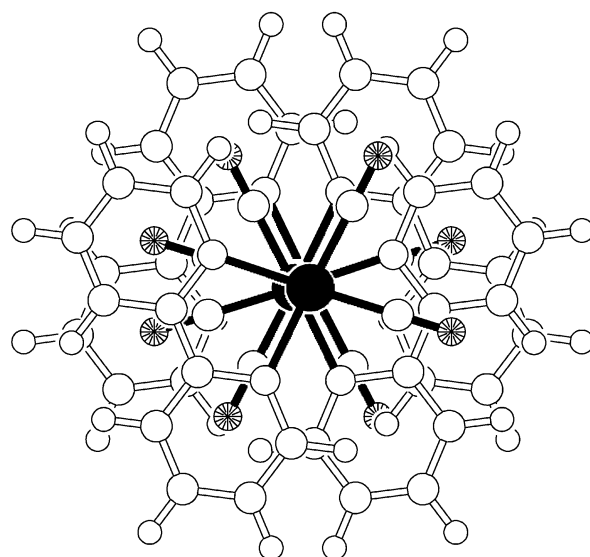
hampering the detection of the actual, *conditioned*, stacking sequence.

XRPD can sometimes afford more information than the pure structure. Indeed, the width of the 001 peak [ca. $1.2^\circ(2\theta)$] suggests an average chain length of ca. 60 Å, i.e. of ca. 20 Ru–Ru bonds. Thus, much shorter chains than in $[\text{Ru}(\text{CO})_4]_n$ (ca. 500 Å) are present.

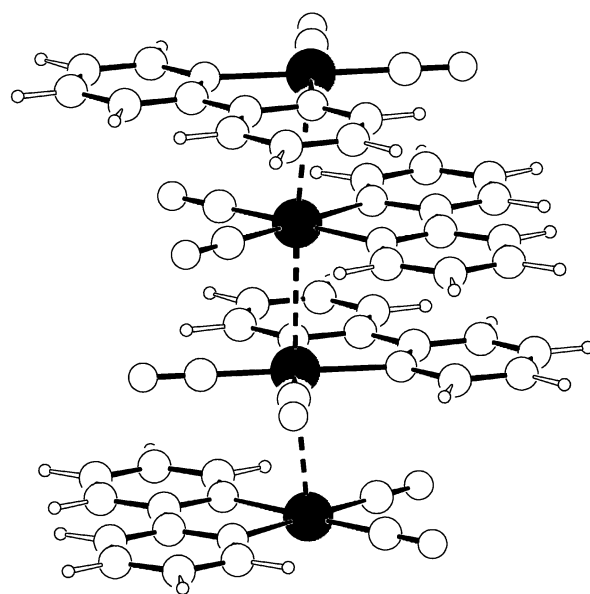
Conclusions

Our results “confirm” the polymeric structure of the samples, with Ru–Ru distances longer than in $[\text{Ru}(\text{CO})_4]_n$; we have shown how these molecules are packed in-plane, demonstrating that flat monomers, staggered by 45 or 135° rotations (as in $[\text{Ru}(\text{CO})_4]_n$), stack in random sequence along the chain; furthermore, for $[\text{Ru}(\text{bpy})(\text{CO})_2]_n$, we have also derived a rough estimate of the average chain length (~ 60 Å).

Obviously, our results do not afford atomic resolution; they are heavily based upon ideal molecules of known geometry; however, despite the very poor diffraction pattern of these species, important crystallochemical results have been obtained by a combination of rather unconventional XRPD methods (“manual” cell determination; database knowledge; direct space structure solution by simulated annealing technique; rigid body refinement; anisotropic modeling of diffraction peak



(a)



(b)

Figure 5. (a) View down $[001]$ of four $[\text{Ru}(\text{bpy})(\text{CO})_2]$ monomers, each one staggered by 135° or 45° with respect to its neighbors. Loss of order down the chain (i.e. random staggering) generates crystallographically disordered chains, resulting in an average mmm symmetry. (b) Side view of an idealized fragment of the $[\text{Ru}(\text{bpy})(\text{CO})_2]_n$ chain, with 135° or 45° staggered monomers; the Ru–Ru bond distances (fragmented lines) are ca. 2.95 Å.

widths; etc.), which could be easily combined in the final model definition with the aid of newly available powerful software.

Acknowledgment. We thank the Italian MURST (COFIN2000, Project “Metal Clusters, Basic and Functional Aspects”) and CNR-ISTM for financial support. We also acknowledge Drs. A. Kern and A. Coelho (Bruker AXS) for providing the β version of the highly performing Topas-R program.

OM020298X